

# On the difficulties for reliable measurements of convection in large aspect ratio Rayleigh-Bénard cells

Christian Kästner, Christian Resagk, Christian Cierpka\*, Jörg Schumacher

Technische Universität Ilmenau, Institute of Thermodynamics and Fluid Mechanics, Ilmenau, Germany

\*corresponding author: christian.cierpka@tu-ilmenau.de

## Abstract

Heat transfer through natural turbulent thermal convection is an important mechanism in geophysics and many engineering problems. A canonical well known experiment is the Rayleigh-Bénard (RB) cell, which consists of an enclosure with adiabatic side walls heated from below and cooled from above. Due to the temperature difference, differences in the density of the fluid cause natural convection. The direct correlation between momentum and heat transfer is currently under investigation especially for large aspect ratios. In this situation one dominant large-scale circulation roll, as typically for low aspect ratios, is substituted by a whole pattern of long-living rolls (Pandey et al., 2018). Nowadays, commonly advanced optical methods are applied to investigate the velocity fields, which makes a transparent heating or cooling plate necessary (Kähler et al., 2016). For the current study glass plates were coated with a thin metal oxide layer enabling heating via the Joule effect. However, since the temperature homogeneity is crucial for the setup, two heating plates had to be combined to enable a homogeneous temperature distribution at the bottom of the convection cell. Additional difficulties arise from the large aspect ratio and thus the large observation angle which may cause optical aberrations and systematic errors due to the perspective bias. Furthermore, the observation duration has to be in the order of minutes to hours to resolve the dynamics of the slowly evolving large-scale flow, which gives additional challenges for the seeding generation.

To prove the reliability of the experimental approach, a convection cell with an aspect ratio  $\Gamma = l/h = 10$  was placed in the SCALEX (Scaled Convective Airflow Laboratory Experiment) facility which enables experiments with SF<sub>6</sub> and air under pressures of up to 10 bar to achieve very high Rayleigh numbers (Körner et al., 2015). Stereoscopic particle image velocimetry (PIV) in horizontal planes covering the whole cross section of the cell ( $300 \times 300 \text{ mm}^2$ ) was used for the estimation of the three components of the velocity vector. The optical access for the laser light sheet was provided by transparent sidewalls. The aim of the current study was to prove the possibility of reliable PIV measurements with reproducible homogenous temperature boundary conditions in the SCALEX facility. Issues of the temperature distribution on the heating plate, tracer particles, illumination and data evaluation will therefore be addressed in greater detail in the following.

## 1 Introduction

In many engineering and natural flow phenomena heat transfer plays an important roles. One prominent example of such a flow configuration is the Rayleigh-Bénard cell. In this canonical example a box is formed by a bottom plate which temperature is set to a higher value in comparison to the top plate. The side walls are modelled to be adiabatic. In that flow configuration heat is transferred to the fluid at the bottom of the cell and consequently its density becomes smaller than the surrounding fluid. Due to the buoyancy a flow might establish that transports heat due to convection from the bottom to the top. The regime is usually described by the Rayleigh number  $Ra = \alpha \Delta T g h^3 / \nu \kappa$ , that relates flow favoring effects and flow hindering effects.  $\alpha$  denotes the thermal expansion coefficient,  $\Delta T$  the temperature difference between hot and cold plate,  $g$  the gravitational acceleration,  $h$  the height of the cell,  $\nu$  the kinematic viscosity and  $\kappa$  the thermal

diffusivity. A convective flow is established for  $Ra > 1708$ . With increasing Rayleigh number the flow state gets more and more complex reaching eventually fully turbulent flow. Of special interest in recent years are flow configurations for large aspect ratios  $\Gamma = L/h$  ( $L$  is the length or diameter of the cell and  $h$  its height) which show a multitude of so called super structures (Pandey et al., 2018). However, up to now only a few large aspect ratio experiments of thermal convection in air have been conducted. They were limited either to smoke visualizations of roll structures (Willis et al. 1972) or pointwise hot-wire measurements (Fitzjarrald 1976). With the current setup it is the aim to allow for a precise measurement of flow structures with optical methods at large Rayleigh numbers and large aspect ratios.

## 2 Experimental Setup

Cell design: The flow structures in large aspect ratio RB cells can be measured in horizontal planes. However, due to the necessary wide field of view the optical access through either the heating plate of the cooling plate is crucial, as was shown in previous studies (Kästner et al., 2017). To allow also for large range in the Rayleigh number, the convection cell was placed in the so called SCALEX facility (Scaled Convective Airflow Laboratory Experiment) at TU Ilmenau. The facility is schematically shown in Fig. 1 an consists of a pressure vessel allowing for the compression of the working fluids (air or sulfur hexafluoride) of up to 10 bar which enables Rayleigh numbers of up to  $10^9$ . The temperature of the interior of the pressure vessel can be precisely be controlled. Details on the facility itself and the control of all experimental parameters can be found in Körner et al. (2015).

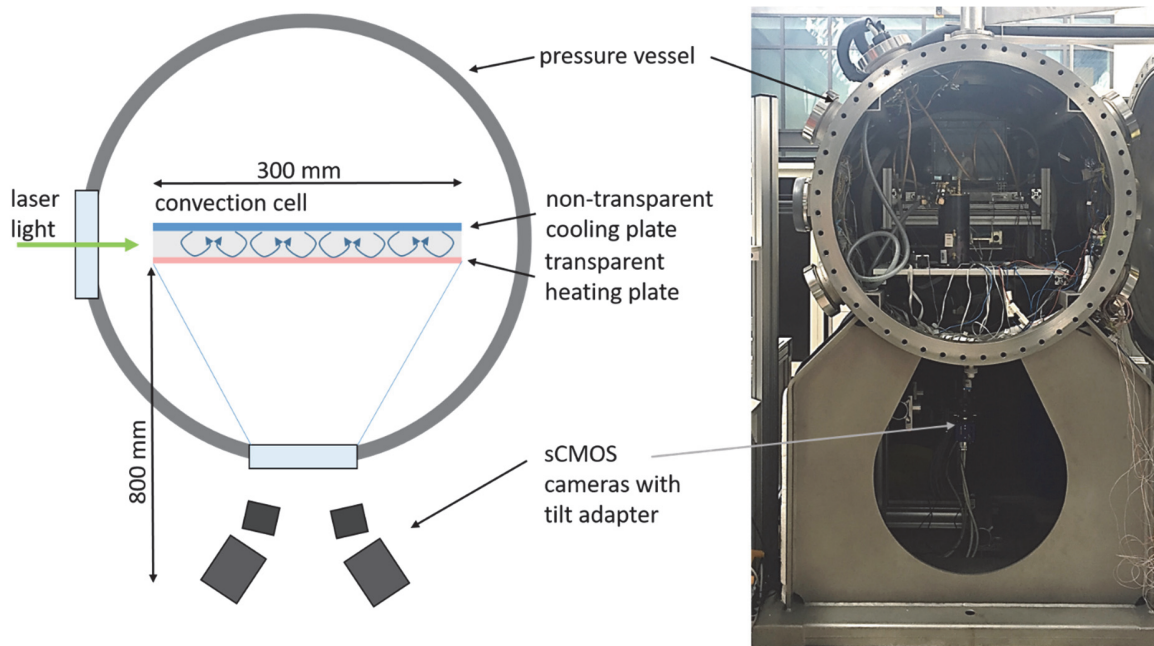


Figure 1: Schematic SCALEX facility and the optical setup for stereoscopic PIV (left) and photograph of the facility from outside the pressure vessel (right).

Optical access is granted by two thick (40 mm) glass windows at the circumference. The convection cell for the current experiment had dimensions of  $300 \times 300 \times 30 \text{ mm}^3$  ( $L \times L \times h$ ) implying some difficulties for the imaging as will be discussed later. The transparent sidewalls were made of 4 mm thick polycarbonate, enabling the illumination by laser light. The aluminum cooling plate is non-transparent and was temperature controlled by a recirculating cooler. The transparent heating plate was arranged using two window pane plates of  $500 \times 500 \times 4 \text{ mm}^3$  size, with one side coated with a thin layer of indium tin oxide (ITO) by plasma deposition. These plates were manufactured at the Fraunhofer Institute for Organic Electronics, Electron Beam and Plasma Technology FEP Dresden (Germany). Ohmic heating was established by contacting the

plates with copper flat bands pushed on the ITO surface with an adjustable DC power supply. In total four different plates were produced and tested with temperature sensors and infrared thermometry on their thermal homogeneity. The best homogeneity was established using two heating plates showing temperature gradients in opposite directions. Both plates were combined in a double glazing, which has the additional advantage of a larger thermal capacity to buffer small thermal fluctuations. The standard deviation of the infrared measurements of the heating plate configuration is shown in Fig. 2 and scales linearly with the temperature. Normalized to the mean temperature it reaches values of up to 3% for a wall temperature of 90°C. To test the applicability of the SCALEX and the measurement system towards compression of the working gas (air) two separate experiments were conducted at a Rayleigh number of  $Ra = 2 \times 10^4$ , first at standard pressure of about 1 bar and 8.1 K temperature difference between heating and cooling plate and second at 2 bar and 1.9 K temperature difference. However, for the current test cases the heating plate was set to temperatures of 25.1°C and 21.9°C which gives a maximum standard deviation of  $< 0.17$  K over the whole test section. More details on the heating plate configuration can be found in Kästner et al., (2017, 2018).

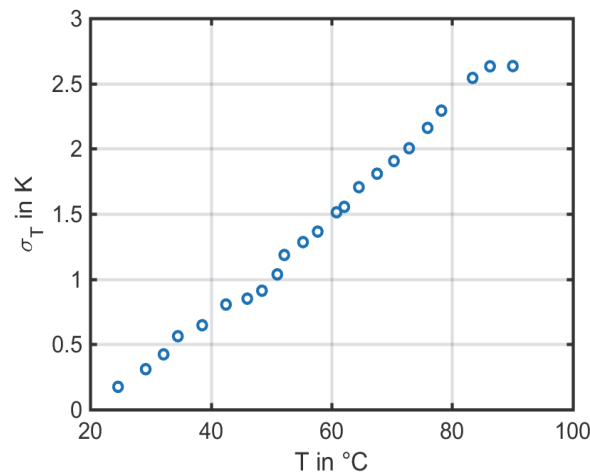


Figure 2: Standard deviation for the temperature fluctuation over the heating plate normalized with the mean temperature.

Seeding: Seeding particles that follow the fluid flow faithfully are necessary for optical measurement techniques. The sedimentation velocity  $u_s$  of the tracer particles can be estimated to be:  $u_s = \frac{d_p^2(\rho_p - \rho_F)}{18\mu} g$ , where  $d_p$  is the particle diameter,  $(\rho_p - \rho_F)$  is the density difference between particle and fluid and  $\mu$  is the dynamic viscosity (Raffel et al., 2018). For a negligible difference in the density the sedimentation velocity becomes also negligible. However, as for gas flows the difference in density using liquid or solid seeding particles is quite high, usually very small particles are used. Therefore the seeding was generated with a vaporizer (PIVTEC GmbH) and consisted of small ( $d_p \sim 1 \mu\text{m}$ ) droplets of di(2-ethylhexyl) sebacate (DEHS). The sedimentation velocity was approximately to be  $u_s = 0.03$  mm/s. The ratio between the natural sedimentation velocity of the particles to the mean velocity of the flow was estimated to be smaller than 0.005 using the average root mean square velocity magnitude calculated from previous simulation. The seeding generator was placed inside the pressure vessel. Control of the magnetic valve was established from outside and allowed an operation under pressure. Tests for pressures of up to 9 bar showed, that small seeding droplets can be generated also for this extended parameter range of the SCALEX facility. With adding the seeding into the convection cell usually momentum is also added to the flow, which disturbs the natural flow state. Therefore the seeding was injected by six distributed ports in the small convection cell from a larger volume (settling chamber) where the seeding can calm down in a as shown in Fig. 3. Additionally, the data acquisition was started approximately 15 minutes after seeding injection to allow the

natural convection to reestablish and minimizing effects due to the added momentum. However, the measurement time is limited to about 120 minutes, due to the evaporation of the seeding droplets. For the current Rayleigh number this translates to about 10,000 to 22,000 free-fall time units, which is enough for a high statistical convergence as will be shown later.

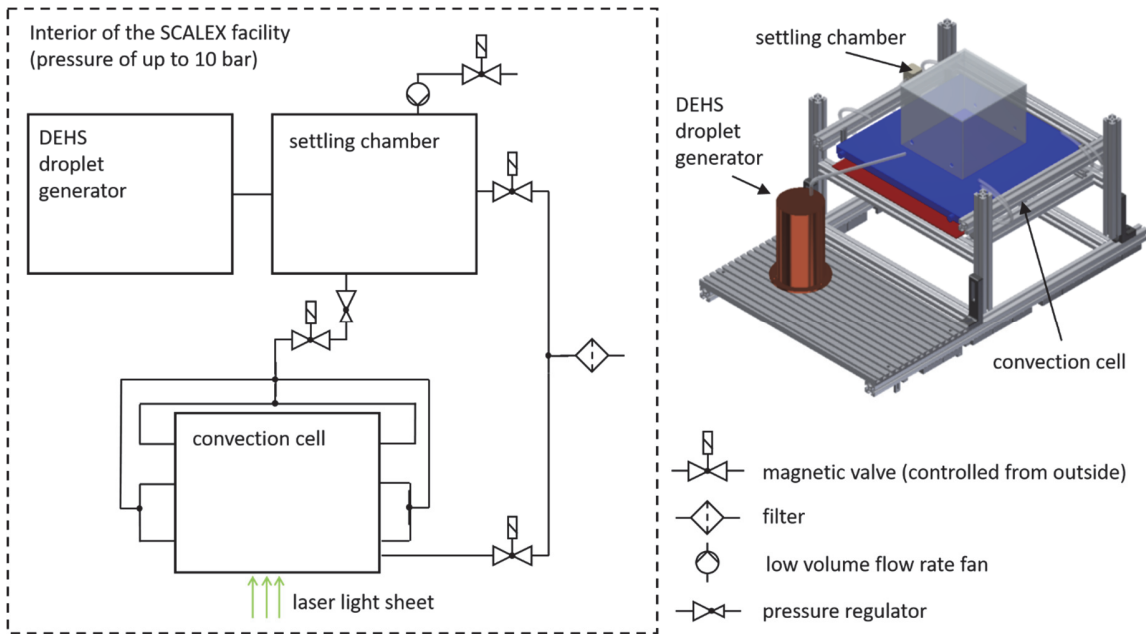


Figure 3: Schematic of the seeding injection configuration for low momentum input in order not to disturb the flow in the test section.

**Data evaluation:** One major challenge for the measurements in Rayleigh-Bénard convection is the fact that all velocity components are in the same order of magnitude. This has two implications for PIV using light sheets. Since for a valid correlation a considerable amount ( $\sim 75\%$ ) of particles should remain in the illuminated area, this limits the time difference between successive images. However, if correlation values of 0.5 ( $\sim 50\%$  particles remain in the volume) would be considered valid, this translates for a 1 mm light sheet to a maximal displacement of 0.5 mm in all directions. Since the absolute error can be estimated to be in the order of 0.05 pixel for carefully adjusted experiments (Raffel et al., 2018), this would give in the current case with a magnification of 0.15 pixel/mm an absolute uncertainty of 0.33 mm, or a relative uncertainty of 66%. Therefore, in order to minimize the relative error in the measurement, longer time differences are preferable. This can be achieved with increasing light sheet thickness for the sake of spatial averaging. Therefore, in the current setup light sheet thicknesses of approximately 1 mm and 5 mm in the field of view (FOV) were used. Using again 50% of particles in the volume the relative uncertainty reduces to 13%. The laser light sheet was created with a double pulse laser (Quantel Q-smart Twins 850) with about 300 mJ pulse energy for the 5 mm thick light sheet and 80 mJ for the 1 mm thin light sheet. Double frame images were recorded with 3.33 Hz and varying pulse separation times since the velocity magnitude of the flow differs for both experiments. The pulse separation at 1.9 K temperature difference was set to the maximum possible pulse separation time of 19.5 ms and to 10 ms for 8.1 K.

Due to limitations in space and optical accessibility the camera had to be placed in a distance of only 0.8 m from the measurement plane. As can be seen in Fig.1, this results in an observation angle of  $\alpha \sim 20^\circ$  which can lead to a significant bias for the in-plane velocity measurement in case of particle motion normal to the observation plane (perspective error, see Raffel et al., 2018). Since the motion normal to the light sheet is random in time and space for the Rayleigh-Bénard configuration, the bias error cannot be corrected. For the out-of-plane motion  $dz = 0.25 \times z_L$ , with  $z_L$  being the light sheet thickness can be estimated. Assuming similar magnitudes for all velocity components, this translates to an uncertainty of 18% for the in-plane

velocity in the worst case (in the edges of the FOV). To avoid this bias, two cameras were used for stereoscopic PIV. Although the angle between the cameras is with  $\sim 24^\circ$  far from being optimal, this setup is the only way to correct for the perspective error.

For the calibration a 3D calibration plate ( $20 \times 20$  cm<sup>2</sup>, LaVision) was placed in the center position of the two measurement planes of the convection experiment and a pin-hole model was applied to map the coordinate system. Additionally, a stereoscopic self-calibration was performed to further reduce uncertainties in the calibration (Wieneke, 2005). A minimum image (which was taken over 10,000 images) was subtracted from each individual image to increase contrast and reduce the background. Since the particle images appear very small on the camera sensor ( $D_p \sim 1.5$  pixels) in the first measurements peak locking was realized to be very pronounced. Especially when the overall displacement is low as in the case for the small light sheet thickness. This effect would give completely wrong velocity probability density functions. Therefore, the cameras were slightly set out of focus to enlarge the particle images on the sensor, which helped to reduce the peak locking effect significantly. The preprocessed images were evaluated using an iterative multigrid cross correlation analysis starting with an interrogation window size of  $128 \times 128$  pixels down to  $32 \times 32$  pixels with 50% overlap.

### 3 First Results

The lifetime of typical structures in RB flows is very long and can be attributed to the free-fall time units  $t_f = h/u_f$ , where  $u_f = \sqrt{\alpha \Delta T g h}$  is the free-fall velocity. Therefore, in Fig. 4 the temporal evolution of the mean values in the center plane over an area of  $-0.75 < x/h < 0.75$  and  $-0.75 < y/h < 0.75$  is shown together with a typical vector field in the center plane using the larger light sheet thickness of 5 mm for ambient pressure and a temperature difference of 8K. It can clearly be seen, that statistical convergence can be reached as the mean values converge. However, averaging time spans of  $\sim 4000 t_f$  are necessary to reach a convergence of 10%. However, for the long measurement times the faster evaporation of the seeding droplets especially for larger pressures are problematic and might render solid seeding particles in the case of SF6 at high pressure necessary.

Nevertheless, the large scale structures are clearly evident by the magnitude of the velocity and the vector fields on the right side of the figure. It can also be seen, that regions of comparably large velocity magnitude are directly adjacent to almost stagnant regions. To highlight the difficulties concerning the light sheet thickness and time difference between two images, the inset shows the histogram for the particular vector field. Peak locking is not observed, however, the small particle image displacements (mean displacement  $\sim 1.5$  pixel) result in a higher mean uncertainty for the in-plane components of about  $\sim 3\%$  but allows a robust

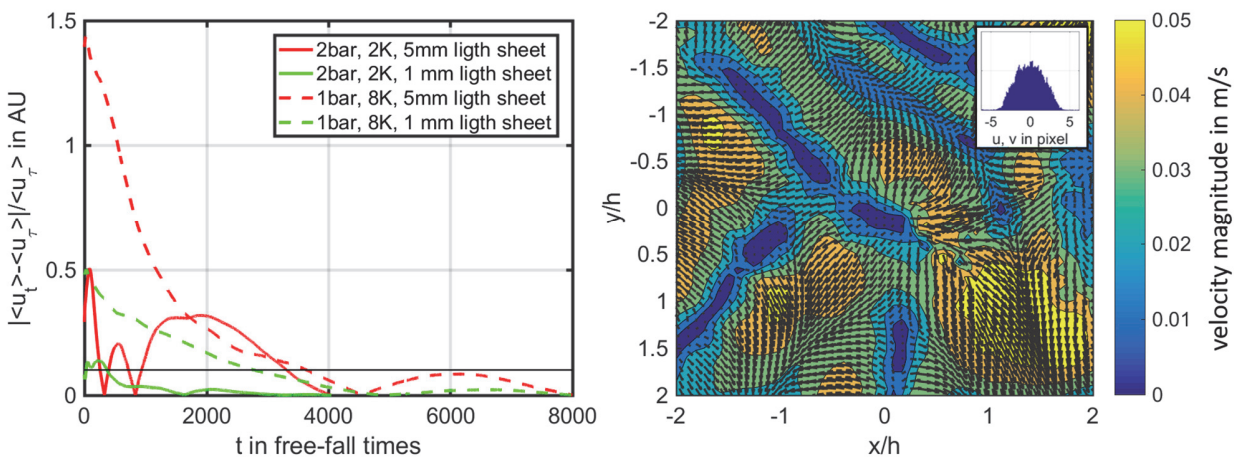


Figure 4: Mean values of the in-plane velocity components in the middle of the convection cell over free fall time units (left) and vector field with the magnitude of the in-plane velocity for a pressure of 1 bar and a temperature difference of 8K using a 5mm thick light sheet (right).

correlation since most of the particles ( $\sim 95\%$  based on the mean in-plane displacement,  $\sim 70\%$  based on the maximum in-plane displacement) remain within the light sheet between the successive illuminations.

## 4 Conclusion

An optically accessible Rayleigh-Bénard convection cell was set up in the SCALEX facility. The optical access of the whole horizontal plane is granted by a transparent heating plate. A seeding system was designed to allow for a seeding without disturbing the natural flow inside the pressurized vessel. First velocity measurements showed, that the stereoscopic arrangement of the cameras reduce the bias due to the perspective error at typically for a large observation angle. A rather thick light sheet allowed to reduce the relative error of the velocity estimation in the complex situation of all velocity components having the same order of magnitude.

## Acknowledgements

The authors acknowledge financial support by the Deutsche Forschungsgemeinschaft DFG under grant no. Re 1066/17-1 and SCHU 1410/18-1, and by the Priority Program on Turbulent Superstructures with Grant No. DFG SPP 1881. The authors are grateful to A. Thieme for technical support and assistance in construction of the convection experiment and the infrared and PIV measurements. The Tesla K40 graphics board used for PIV analysis was donated by the NVIDIA Corporation.

## References

- Emran MS, Schumacher J (2015) Large-scale mean patterns in turbulent convection. *Journal of Fluid Mechanics* 776:96-108, DOI: 10.1017/jfm.2015.316
- Fitzjarrald DE (1976) An experimental study of convection in air. *Journal of Fluid Mechanics* 73:693-719, DOI: 10.1017/S0022112076001572
- Kähler CJ, Astarita T, Vlachos PP, Sakakibara J, Hain R, Discetti S, La Foy R, Cierpka C (2016) Main results of the 4th International PIV Challenge. *Experiments in Fluids* 57:97, DOI: 10.1007/s00348-016-2173-1
- Kästner C, Resagk C, Westphalen J, Junghänel M, Cierpka C, Schumacher J (2018) Assessment of horizontal velocity fields in square thermal convection cells with large aspect ratio, *Experiments in Fluids*, under review
- Kästner C, Resagk C, Baczyzmalski D, Massing J, Moller S, Kähler CJ, Schumacher J, Cierpka C (2017) Heat and mass transport in large aspect ratio Rayleigh-Bénard convection, 9th World Conference on Experimental Heat Transfer, Fluid Mechanics and Thermodynamics, July 12-15, Iguazu Falls, Brazil
- Körner M, Resagk C, Thess A (2015) Large-scale structures in mixed convection. 15th European Turbulence Conference, August 25-28, Delft, The Netherlands
- Pandey A, Scheel JD, Schumacher J (2018) Turbulent superstructures in Rayleigh-Bénard convection, *Nature Communications* 9, 2118, DOI: 10.1038/s41467-018-04478-0
- Wieneke B (2005) Stereo-PIV using self-calibration on particle images, *Experiments in Fluids* 39, 267–280, DOI: 10.1007/s00348-005-0962-z
- Willis GE, Deardorff JW, Somerville RCJ (1972) Roll-diameter dependence in Rayleigh convection and its effect upon the heat flux. *Journal of Fluid Mechanics* 54:351-367, DOI: 10.1017/S0022112072000722